Process for Preparing Macroscopic Quantities of Brightly Photoluminescent Silicon Nanoparticles with Emission Spanning the Visible Spectrum

Xuegeng Li, Yuanqing He, Suddha S. Talukdar, and Mark T. Swihart*

Department of Chemical Engineering, University at Buffalo (SUNY), Buffalo, New York 14260-4200

Silicon nanoparticles with bright visible photoluminescence have been prepared by a new combined vapor phase and solution phase process, using only inexpensive commodity chemicals. CO_2 laser induced pyrolysis of silane was used to produce Si nanoparticles at high rates (20−200 mg/h). Particles with an average diameter as small as 5 nm were prepared directly by this vapor phase (aerosol) synthesis. Etching these particles with mixtures of hydrofluoric acid (HF) and nitric acid (HNO_3) reduced the size and passivated the surface of these particles such that after etching they exhibited bright visible luminescence at room temperature. The wavelength of maximum photoluminescence (PL) intensity was controlled from above 800 nm to below 500 nm by controlling the etching time and conditions. Particles with blue emission (maximum PL intensity at 420 nm) were prepared by rapid thermal oxidation of orange-emitting particles. The particle synthesis methods; steady-state photoluminescence spectra; results of their characterization using TEM, XRD, FTIR absorption spectroscopy, and XPS; and preliminary assessments of the stability of the photoluminescence properties with time are presented here. Preparation of macroscopic quantities by the methods described here opens the door to chemical studies of free silicon nanoparticles that could previously be carried out only on porous silicon wafers, as well as to potential commercial applications of silicon nanoparticles.

1. Introduction

The possibility of constructing optoelectronic devices, full-color displays, and optical sensors based on silicon has generated tremendous interest in the preparation and characterization of light emitting silicon nanoparticles. Because the particles' luminescence properties are size-dependent, multiple colors can be produced using a single material. These particles also have exciting potential applications as fluorescent tags for biological imaging, as has been proposed for II−VI compound semiconductor nanoparticles.[1−3] They can be brighter and much more stable to photobleaching than the organic dyes used in these applications, and they also have much broader excitation spectra, so that emission at multiple wavelengths (from particles of different sizes) can be excited by a single source. There are established methods for preparation of luminescent porous silicon,[4] and aerosol synthesis of macroscopic quantities of nonluminescent silicon nanoparticles has been known for over 20 years.[5,6] However, there are, to our knowledge, no reported methods for producing macroscopic quantities (i.e,. more than a few milligrams) of luminescent silicon nanoparticles that are free from a substrate. Soon after the initial discovery of photoluminescence from porous silicon,[7] Brus and co-

workers published a series of papers[8−11] in which they prepared silicon nanoparticles by high-temperature decomposition of disilane. These studies were instrumental in building understanding of photoluminescence mechanisms in silicon nanostructures. However, in their actual particle synthesis experiments, they collected less than 10 mg of particles per 24 h day of reactor operation.[9] Carlisle et al.[12,13] and other groups have prepared small quantities of luminescent silicon nanoparticles by laser vaporization controlled condensation (LVCC). Recently, Korgel and co-workers prepared brightly luminescent silicon nanoparticles in supercritical organic solvents at high temperature (500 °C) and pressure (345 bar).[14−16] Again, they have produced beautiful and well-characterized particles, but in quite small quantities. In their first report,[16] 0.2 mL per batch of 250−500 mM diphenylsilane was converted to silicon nanoparticles with a yield of 0.5%−5%, which corresponds to 0.07−1.4 mg of Si nanoparticles per batch. Nayfeh and co-workers, as well as a number of other groups, have produced brightly luminescent silicon nanoparticles by dislodging them from luminescent porous silicon wafers prepared electrochemically,[17−19] and this has also generated tremendous tech-

---

* Corresponding author. Phone: (716) 645-2911, ext 2205. Fax: (716) 645-3822. E-mail: swihart@eng.buffalo.edu.
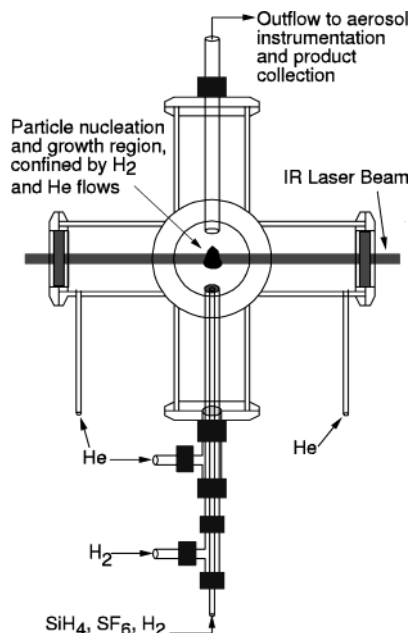(1) Chan, W. C. W.; Nie, S. *Science* **1998**, *281*, 2016−2018.
(2) Bruchez, M., Jr.; Moronne, M.; Gin, P.; Weiss, S.; Alivisatos, A. P. *Science* **1998**, *281*, 2013−2015.
(3) Lacoste, T. D.; Michalet, X.; Pinaud, F.; Chemla, D.; Alivisatos, A. P.; Weiss, S. *Proc. Natl. Acad. Sci. U.S.A.* **2000**, *97*, 9461−9466.
(4) *Light Emission in Silicon From Physics to Devices* Lockwood, D. J., Ed.; Academic Press: New York, 1998.
(5) Cannon, W. R.; Danforth, S. C.; Flint, J. H.; Haggerty, J. S.; Marra, R. A. *J. Am. Ceram. Soc.* **1982**, *65*, 324−330.
(6) Cannon, W. R.; Danforth, S. C.; Haggerty, J. S.; Marra, R. A. *J. Am. Ceram. Soc.* **1982**, *65*, 330−335.
(7) Canham, L. T. *Appl. Phys. Lett.* **1990**, *57*, 1046−1048.

(8) Wilson, W. L.; Szajowski, P. J.; Brus, L. *Science* **1993**, *262*, 1242−1244.
(9) Littau, K. A.; Szajowski, P. J.; Muller, A. J.; Kortan, A. R.; Brus, L. *J. Phys. Chem.* **1993**, *97*, 1224−1230.
(10) Brus, L. *J. Phys. Chem.* **1994**, *98*, 3575−3581.
(11) Brus, L. E.; Szajowski, P. J.; Wilson, W. L.; Harris, T. D.; Schuppler, S.; Citrin, P. H. *J. Am. Chem. Soc.* **1995**, *117*, 2915−2922.
(12) Carlisle, J. A.; Dongol, M.; Germanenko, I. N.; Pithawalla, Y. B.; El-Shall, M. S. *Chem. Phys. Lett.* **2000**, *326*, 335−340.
(13) Carlisle, J. A.; Germanenko, I. N.; Pithawalla, Y. B.; El-Shall, M. S. *J. Electron Spectrosc.* **2001**, *114−116*, 229−234.
(14) Ding, Z. F.; Quinn, B. M.; Haram, S. K.; Pell, L. E.; Korgel, B. A.; Bard, A. J. *Science* **2002**, *296*, 1293−1297.
(15) English, D. S.; Pell, L. E.; Yu, Z. H.; Barbara, P. F.; Korgel, B. A. *Nano Lett.* **2002**, *2*, 681−685.
(16) Holmes, J. D.; Ziegler, K. J.; Doty, R. C.; Pell, L. E.; Johnston, K. P.; Korgel, B. A. *J. Am. Chem. Soc.* **2001**, *123*, 3743−3748.

nological and scientific interest. However, this method also generates small quantities of silicon nanocrystals, and the emitting nanocrystals may be embedded in larger porous silicon particles.

The first solution phase synthesis of Si nanoparticles was presented by Heath.[20] More recently Kauzlarich and co-workers have demonstrated several procedures[21–24] for producing silicon nanoparticles with a variety of surface terminations at mild conditions in solution using reactive Zintl salts. They are able to produce larger quantities of particles than the methods described in the previous paragraph. In some cases, they have shown blue-UV photoluminescence (PL) from these particles, but appear not to have observed the orange to red PL characteristic of porous silicon and most other nanoparticle preparation methods, including that presented here. Solid phase reactions have also been used to produce larger quantities of silicon nanoparticles, but apparently with much lower PL efficiency than the particles mentioned in the previous paragraph. Lam et al.[25] produced silicon nanoparticles by the reaction of graphite with SiO_2 in a ball mill. A wide range of particle sizes were produced, but some PL was observed after ball milling for 7–10 days. Ostraat and co-workers have prepared oxide-capped silicon nanoparticles via vapor phase decomposition of highly diluted SiH_4 in nitrogen[26,27] followed immediately by surface oxidation.

CO_2 laser pyrolysis of silane is an effective method of producing gram-scale quantities of silicon nanoparticles, as first shown more than 20 years ago.[5,6] It produces high-purity loosely agglomerated particles with controlled primary particle size and size distribution. Moreover, it is a continuous process that permits reasonable production rates. While several groups have synthesized silicon particles with this and similar methods, the resulting particles showed little or no visible photoluminescence.[28–30] An exception to this is the work of Huisken and co-workers,[31–35] who use pulsed CO_2 laser pyrolysis of silane, which yields luminescent particles, but in very small quantities, and have studied the effect of particle aging in air and surface etching with HF on the photoluminescence spectrum.[35]

(17) Nayfeh, M. H.; Barry, N.; Therrien, J.; Akcakir, O.; Gratton, E.; Belomoin, G. *Appl. Phys. Lett.* **2001**, *78*, 1131–1133.

(18) Nayfeh, M. H.; Akcakir, O.; Belomoin, G.; Barry, N.; Therrien, J.; Gratton, E. *Appl. Phys. Lett.* **2000**, *77*, 4086–4088.

(19) Belomoin, G.; Therrien, J.; Smith, A.; Rao, S.; Twesten, R.; Chaieb, S.; Nayfeh, M. H.; Wagner, L.; Mitas, L. *Appl. Phys. Lett.* **2002**, *80*, 841–843.

(20) Heath, J. R. *Science* **1992**, *258*, 1131–1133.

(21) Baldwin, R. K.; Pettigrew, K. A.; Ratai, E.; Augustine, M. P.; Kauzlarich, S. M. *Chem. Commun.* **2002**, *17*, 1822–1823.

(22) Bley, R. A.; Kauzlarich, S. M. *J. Am. Chem. Soc.* **1996**, *118*, 12461–12462.

(23) Liu, Q.; Kauzlarich, S. M. *Mater. Sci. Eng. B* **2002**, *B96*, 72–75.

(24) Mayeri, D.; Phillips, B. L.; Augustine, M. P.; Kauzlarich, S. M. *Chem. Mater.* **2001**, *13*, 765–770.

(25) Lam, C.; Zhang, Y. F.; Tang, Y. H.; Lee, C. S.; Bello, I.; Lee, S. T. *J. Cryst. Growth* **2000**, *220*, 466–470.

(26) Ostraat, M. L.; De Blauwe, J. W.; Green, M. L.; Bell, L. D.; Atwater, H. A.; Flagan, R. C. *J. Electrochem. Soc.* **2001**, *148*, G265–G270.

(27) Ostraat, M. L.; De Blauwe, J. W.; Green, M. L.; Bell, L. D.; Brongersma, M. L.; Casperson, J.; Flagan, R. C.; Atwater, H. A. *Appl. Phys. Lett.* **2001**, *79*, 433–435.

(28) Borsella, E.; Falconieri, M.; Botti, S.; Martelli, S.; Bignoli, F.; Costa, L.; Grandi, S.; Sangaletti, L.; Allieri, B.; Depero, L. *Mater. Sci. Eng. B* **2001**, *B79*, 55–62.

(29) Borsella, E.; Botti, S.; Cremona, M.; Martelli, S.; Montereali, R. M.; Nesterenko, A. *J. Mater. Sci. Lett.* **1997**, *16*, 221–223.

(30) Botti, S.; Coppola, R.; Gourbilleau, F.; Rizk, R. *J. Appl. Phys.* **2000**, *88*, 3396–3401.

(31) Ehbrecht, M.; Kohn, B.; Huisken, F.; Laguna, M. A.; Paillard, V. *Phys. Rev. B* **1997**, *56*, 6958–6964.

(32) Huisken, F.; Kohn, B. *Appl. Phys. Lett.* **1999**, *74*, 3776.

(33) Ledoux, G.; Amans, D.; Gong, J.; Huisken, F.; Cichos, F.; Martin, J. *Mater. Sci. Eng.* **2002**, *C19*, 215–218.

Figure 1. Schematic of laser-driven aerosol reactor.

To show efficient visible photoluminescence (PL), it is believed that silicon nanoparticles must be smaller than 5 nm, and their surface must be "properly passivated" such that there are no nonradiative recombination sites on it. The mechanism(s) of photoluminescence in silicon nanocrystals and the effect of surface passivation on light emission from them remain topics of active research and debate. The size of silicon nanoparticles can be reduced by etching them in mixtures of hydrofluoric acid (HF) and nitric acid (HNO_3)[36] as well as by aging them in air and then removing the resulting oxide with HF.[35] We have recently discovered that a controlled HF/HNO_3 etching process can induce bright, visible photoluminescence in silicon nanoparticles produced by laser pyrolysis of silane that do not show significant photoluminescence before etching. In the present contribution, we present this two-step particle synthesis process—laser pyrolysis synthesis followed by acid etching—and the photoluminescence properties of the resulting particles. These photoluminescence properties appear to be very similar to those of both porous silicon and the aerosol-synthesized particles produced in much smaller quantities by Brus and co-workers and Huisken and co-workers as described above. The significance of this contribution is that it enables the production of macroscopic quantities (up to a few hundred milligrams in a few hours in our small bench-scale implementation) of Si nanoparticles with bright visible photoluminescence. Availability of these quantities of particles allows the study of their surface functionalization and of their incorporation into devices that simply is not possible with the smaller quantities of free silicon particles produced by other methods.

2. Experimental Section

The silicon powders were synthesized by laser-induced heating of silane to temperatures where it dissociates, in the reactor shown schematically in Figure 1. A continuous CO_2 laser beam (Coherent, Model 42 laser emitting up to 60 W) was focused to

(34) Ledoux, G.; Gong, J.; Huisken, F.; Guillois, O.; Reynaud, C. *Appl. Phys. Lett.* **2002**, *80*, 4834–4836.

(35) Ledoux, G.; Gong, J.; Huisken, F. *Appl. Phys. Lett.* **2001**, *79*, 4028–4030.

(36) Seraphin, A. A.; Werwa, E.; Kolenbrander, K. D. *J. Mater. Res.* **1997**, *12*, 3386–3392.

a diameter of about 2 mm just above the central reactant inlet, which was made from 1/8 in. o.d. tubing centered within a piece of 3/8 in. o.d. tubing through which a sheath flow of H_2 and/or helium entered the reactor. This sheath gas helps to confine the reaction zone to a small region near the axis of the reactor. The exact dimensions of the reaction zone are difficult to determine, but are probably of order 2 mm in both diameter and thickness. Silane (electronic grade, Scott Gases) weakly absorbs the laser energy at a wavelength of 10.6 μm, and is thereby heated. Sulfur hexafluoride (SF_6) may be added to the precursor stream as a photosensitizer. SF_6 (technical grade, Aldrich) has a large absorption cross section at the laser wavelength and can therefore dramatically increase the temperature achieved for a given laser power. Helium (UHP, passed through an oxygen trap to remove residual O_2 and H_2O) and hydrogen (ultrapure carrier grade) flows confine the reactant and photosensitizer (SF_6) to a region near the axis of the reactor and prevent them from accumulating in the arms of the six-way cross from which the reactor is constructed. Hydrogen also serves to increase the temperature at which particle nucleation occurs, and to decrease the particle growth rate, since it is a byproduct of silane dissociation and particle formation. All gas flow rates to the reactor were controlled by mass flow controllers. The resulting particles were collected on cellulose nitrate membrane filters. The effluent was directed to a furnace where it was heated to 850 °C to decompose any residual silane. Typical experimental conditions were a total pressure of 540 mbar in the reactor; a laser power of 60 W; 24 sccm SiH_4, 2 sccm SF_6, and 100 sccm H_2 flowing through the central inlet (1/8 in. tube); 600 sccm H_2 flowing through the sheath inlet (3/8 in. tube); and 1500 sccm He (total) flowing through the four inlets near the four windows of the reactor.
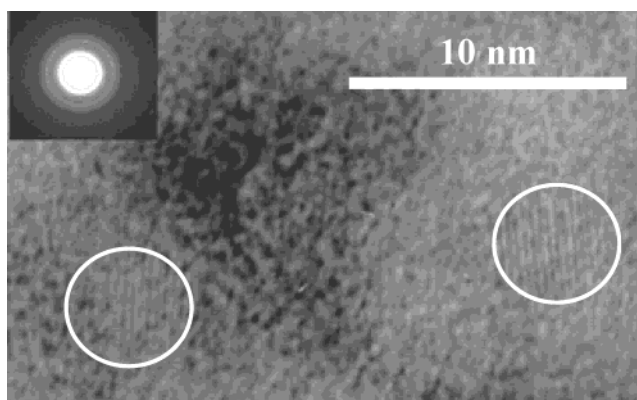
This method can produce silicon nanoparticles at 20−200 mg/h in the present configuration. With a commercially available multi-kilowatt laser focused into a thin sheet, one could readily scale this up by 2 orders of magnitude. By using an array of inlets of approximately the same dimensions as those used here, each surrounded by a sheath flow, it should be possible to mimic the conditions in the laboratory reactor. A possible configuration would be a 22 by 21 hexagonal array of 462 1/8 in. o.d. tubes in which each reactant inlet is surrounded by six sheath flow inlets (100 reactant inlets and 362 sheath inlets). This array would be about 7 cm wide and 6 cm deep. In conjunction with a 6 kW laser expanded into an 8 cm wide by 2 mm thick sheet and appropriate gas flow rates, this would provide a straightforward 100-fold scaleup strategy. Laser power requirements could be reduced by reflecting the beam through the reaction zone multiple times, rather than using a single pass as is done in the laboratory experiments.

The powders obtained as described above were dispersed in methanol using mild sonication, then etched with solutions of 0.5%−20% HF and 10%−40% HNO_3 in water to reduce the particle size and passivate the particle surface. Acid solutions were prepared from 49−51 wt % HF, 68−70% HNO_3, and DI water in the necessary proportions. After etching, the particles were collected on polyvinylidene fluoride (PVDF) membrane filters (Millipore) and washed with DI water and methanol. Depending on etching conditions and initial particle size, 10%−50% of the original particle mass is recovered after this process.

The silicon nanoparticles were characterized by transmission electron microscopy (TEM) and specific surface area measurements (Brunauer−Emmett−Teller method) prior to etching and by TEM after etching. Photoluminescence spectra (fluorescence spectra) were recorded with a Perkin-Elmer LS 50 fluorescence spectrometer with a 351 nm band-pass filter used to suppress any scattered light from the source. The excitation wavelength was set to 355 nm and the emission cutoff filter was set to 430 nm for most of the PL measurements shown here. For emission measurements on blue-emitting particles, the emission cutoff filter was set to 390 nm.

3. Results and Discussion

a. Initial Nonluminescent Nanoparticles. The TEM micrograph (Figure 2) and others like it show that the as-synthesized powder in this case consists of nanocrystals with an average diameter near 5 nm. While many particles such as those shown in Figure 2 are clearly visible in
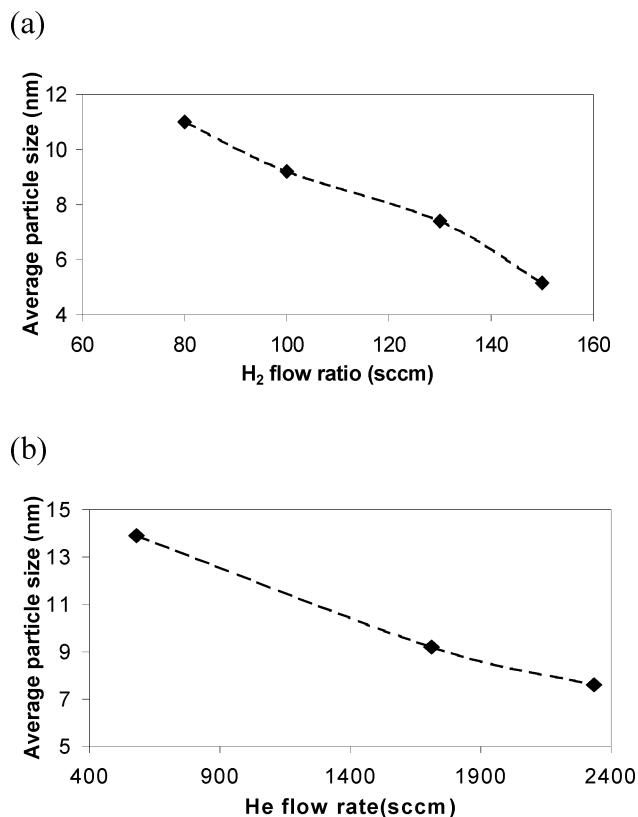

Figure 2. TEM image of silicon nanoparticles before etching. The inset shows the selected area electron diffraction pattern from the particles in the image. Two nanocrystals are circled for ease of identification.

TEM images, the image quality is not high enough to produce meaningful measurements of particle size distribution by particle counting. Selected area electron diffraction patterns obtained from the Si nanoparticles (Figure 2, inset) show that the particles are a mixture of crystalline and amorphous material, or that the crystallites are too small to produce a well-defined diffraction pattern. No special precautions have been taken to avoid beam-induced heating, and the resultant possible melting, of the particles, so this possibility cannot be definitively ruled out.
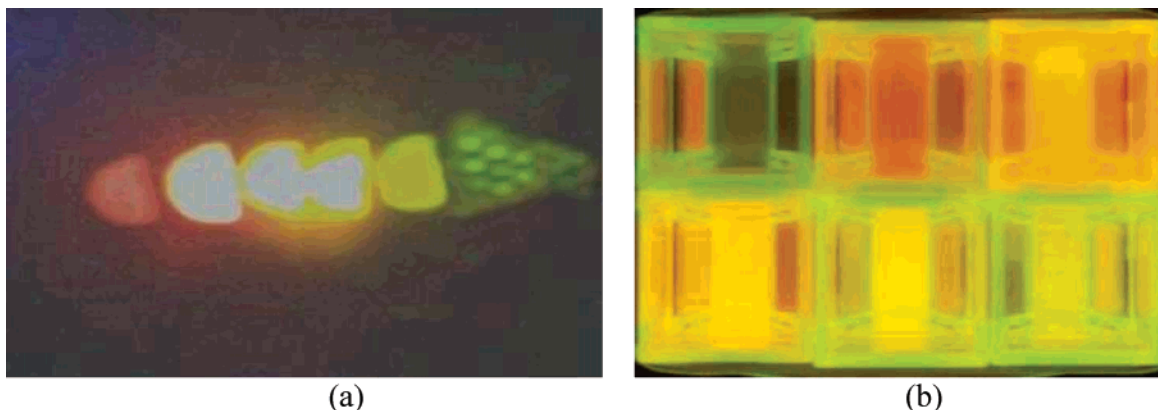
Nitrogen physisorption (the BET method, using Micromeretics Model 2010 ASAP physisorption apparatus) was used to measure the specific surface area of particles. The measured surface area for the sample shown in Figure 2 was 500 m²/g. For spherical particles with the same density as bulk silicon, this is equivalent to a particle diameter of 5.2 nm. This is in close agreement with the TEM images. Particle size, crystallinity, and production rate can be controlled by varying the flow rates of H_2 and He to the reactor and by addition of SF_6. Changing these parameters allows us to produce particles with average diameters in the range of 5−20 nm. Larger particles are also easily produced, but are not presently of interest. Figure 3 shows examples of the dependence of primary particle size on carrier gas flow rates (with SiH_4 flow rate and all other conditions held constant) for typical operating conditions and a total reactor pressure of 8 psia (540 mbar).

b. Photoluminescence Induced by Etching Non-luminescent Particles. Upon initial synthesis in the laser-driven reactor, the silicon nanoparticles exhibit little or no visible photoluminescence (PL) either as a dry powder or dispersed in solvents, although some weak PL in the infrared (beyond 850 nm) cannot be ruled out. After etching with HF/HNO_3 mixtures as described above, the particles exhibit bright visible PL. During the etching process, the nanoparticles are oxidized by HNO_3, and the resulting oxide is dissolved (etched) by HF, so that the size of the silicon core of the particles is reduced, and the surface is passivated with oxide produced by wet oxidation with HNO_3, rather than by the "native oxide" that forms when the particles are exposed to room air. Powder samples and particle dispersions in water, methanol, and other solvents, with bright visible PL ranging from red to green, have been produced as shown in Figures 4 and 5. The emission wavelength decreases smoothly and monotonically with increasing etching time. This apparent size-dependent photoluminescence is comparable to that of the best published examples of silicon nanoparticles produced by electrochemical etching of silicon wafers.[19]

(a)

(b)

Figure 3. Dependence of particle size on carrier gas flow rates for typical reactor conditions. Particle diameter is based on BET surface area measurement. In (a) the H_2 flow plotted is through the central inlet with the SiH_4. Other flow rates are as follows: (a) $SiH_4 = 24$ sccm, He = 1450 sccm, H_2 (outer inlet) = 800 sccm, $SF_6 = 3.2$ sccm; (b) $SiH_4 = 48$ sccm, H_2 (center inlet) = 40 sccm, $SF_6 = 0$ sccm.

In Figures 4 and 5, the peak PL emission wavelength decreases from near 855 nm to 570 nm with increasing etching time. In other samples, we have seen peaks in the PL spectrum at wavelengths below 500 nm after etching. For powder samples and particle dispersions with a peak PL wavelength near 600 nm, the photoluminescence intensity and spectrum are relatively stable. However, preliminary results suggest that, for dispersions of particles in water or methanol and for samples with initial peak PL emission at shorter wavelengths, the spectrum changes with time after the etching procedure. This is further discussed below.

Preliminary attempts were made to measure the external quantum efficiency of the photoluminescence by reference to organic dyes. However, as discussed further below, without surface treatment, the particles do not form stable dispersions in organic solvents. Thus, the particle dispersions (of agglomerated particles) scattered a significant amount of the incoming (excitation) beam. Therefore, when the dye solution and particle dispersion had the same transmission of the incident beam, in fact the particle dispersion was absorbing less light than the dye solution. These experiments gave external quantum efficiencies of about 0.5%−1% at room temperature. However, due to the scattering from agglomerated particles, the true quantum efficiency could be much higher, and this must be regarded as a lower limit. More reliable measurements made on samples that have been functionalized with organic molecules so that they can be well dispersed in organic solvents are underway and will be reported separately. We do not presently have the capability to make quantum yield measurements on powder samples.

To further characterize the crystal structure, elemental concentrations, and particle surface properties, powder X-ray diffraction (XRD), X-ray photoelectron spectroscopy (XPS), and Fourier transform infrared absorption spectroscopy (FTIR) measurements were conducted on powder samples of the luminescent Si nanoparticles.

Figure 6 shows XRD results for the original, nonluminescent particles and luminescent particles with PL peaks centered at 700, 650, and 630 nm. The original and etched samples were all from the same batch of unetched particles. From Figure 6a, the original sample and all three different etched samples show peaks characteristic of crystalline silicon at 2θ values of $\sim$28.3°, 47.2°, and 56.0°. These results confirm that crystalline silicon is present in both original and etched, luminescent particles. If we consider the details of the peak centered at $\sim$28.3°, we find that particles with broader XRD peaks have shorter PL wavelength. If the PL of the etched particles is size-dependent, particles with shorter PL peak wavelength should be smaller. XRD results support this hypothesis. For particles in this size range (less than 10 nm) substantial broadening of the XRD peaks due to finite size effects is expected. The degree of broadening depends on strain and possibly other factors as well as particle size. These particles are expected to be highly strained, due to the presence of a SiO_2 shell on their surface. Therefore, the Scherrer formula cannot reliably be used to determine the particle size. However, the trend of
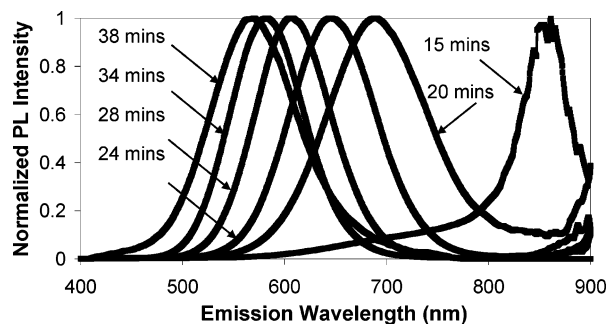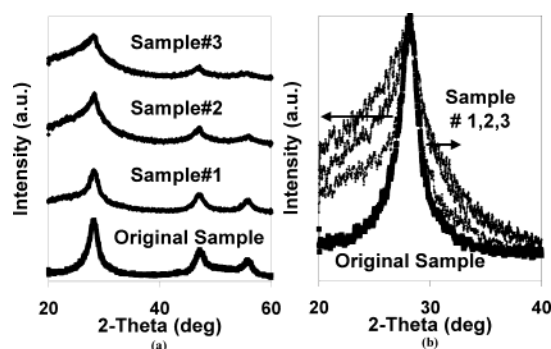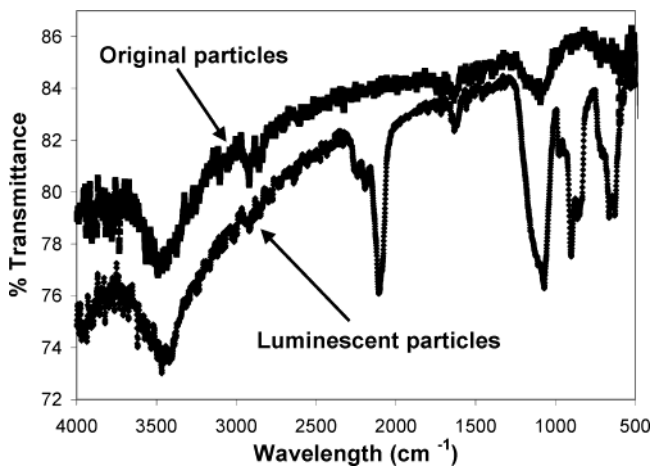

Figure 4. Samples with bright visible PL under UV illumination: (a) powder sample; (b) particles from the same experiment dispersed in methanol. From left to right in (a) and from upper left to lower right in (b) etching time increases, and therefore particle size decreases. The powder samples are illuminated from above, while the dispersions are illuminated from below. Both are photographed from above.

Figure 5. Normalized photoluminescence spectra of dry powder samples shown in Figure 4a, showing the decrease in peak emission wavelength with increasing etching time (and, presumably, therefore with decreasing particle size) in a roughly 3% HF/26% HNO$_3$ etching solution. The sensitivity of the R928 photomultiplier tube used here falls off sharply beyond 800 nm, and this is the source of the noisiness and odd shape of the 15 min spectrum. Spectra have been corrected for detector sensitivity and normalized.

Figure 6. (a) Powder XRD patterns of original and etched silicon nanoparticles (simply called samples 1, 2, and 3). For samples 1, 2 and 3, the peak PL emission wavelengths are 700, 650, and 630 nm, respectively. (b) Normalized XRD peaks at 28.3° for the four samples.

Figure 7. FTIR spectra for original and etched Si particles. The etched particles were washed with 5% HF solution.

increased broadening of the XRD peaks with increasing etching time and decreasing PL wavelength supports the interpretation that the particle size is decreasing with increasing etching time and this shifts the emission wavelength toward the blue.
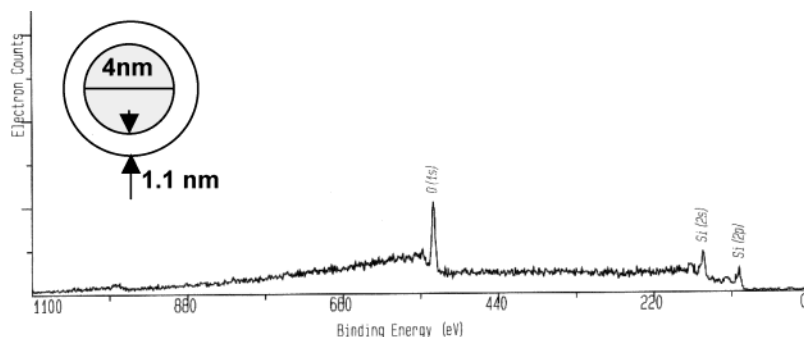
Figure 7 shows FTIR spectra for the same sample before and after being etched and washed with 5% HF solution (etched sample 1 from Figure 6). For both the original and etched samples, there are peaks at ~1070 cm^{-1}, which correspond to Si–O bonds. After etching, there is strong

peak at ~2108 cm^{-1} for Si–H. For the original sample, there is no peak at this position. For other unetched samples, we have observed a weak peak at this Si–H stretching frequency. The Si–O bonds in the original sample presumably come from slow air oxidization, since the particles are prepared in an oxygen-free environment and their as-prepared surfaces could consist of a mixture of H-termination and dangling bonds. Washing with 5% HF as the final step in the etching procedure increased the intensity of the Si–H features, but these features are much larger for etched than for unetched samples even without this step. Clearly, the state of the particle surface changes substantially during the etching process. The surface structure of the luminescent samples is qualitatively different from that of the nonluminescent samples. However, the FTIR spectral features do not correlate with the PL emission wavelength. The FTIR spectra for samples 1, 2, and 3 of Figure 6 are essentially identical. The relative intensities of Si–H and Si–O features change with etching conditions (HNO$_3$ to HF ratio) and with post-etching exposure to either HF or HNO$_3$ alone, but they do not change with total etching time for given conditions and procedure.
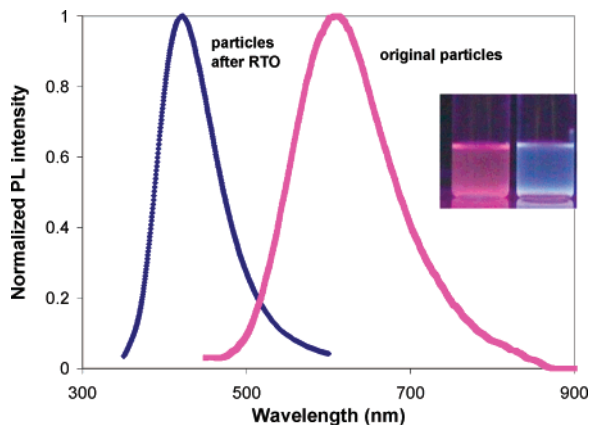
X-ray photoelectron spectroscopy (XPS) was used to determine the elemental composition of the particles. Figure 8 shows the XPS spectrum for the etched sample 1 after exposure to air for 10 days. The XPS spectrum shows peaks only for silicon and oxygen. The atomic percent concentration ratio of Si and O is 45.3:54.7. Using this ratio, we can calculate a volume ratio of SiO$_2$ to Si of 3.45:1 within the 2 nm analysis depth of the experiment (assuming a density of 2.2 g/cm^3 for SiO$_2$ and 2.33 g/cm^3 for Si). If the particles have a spherical core–shell structure with a crystalline silicon core diameter of 4 nm, then this ratio corresponds to an oxide shell about 1.1 nm thick. This degree of oxidation is reasonable for a sample that has been exposed to air for 10 days. Results were similar for sample 2, which had a lower Si to O ratio of 43:57, consistent with a slightly smaller core size or slightly thicker oxide shell. This is consistent with the fact that sample 2 emitted at a shorter wavelength (peak at 650 nm) than sample 1 (peak at 700 nm). Thus, XPS results also support the hypothesis that emission wavelength decreases with decreasing particle size. Furthermore, the XPS elemental analysis is consistent with the picture of Si core/SiO$_2$ shell structures of approximately the size expected.

c. Production of Blue-Emitting Particles by Rapid Thermal Oxidation (RTO). We have not yet produced blue-emitting particles directly from the etching process described above, though it may yet prove possible to do so. However, we have produced blue-emitting particles by rapid thermal oxidization (RTO) of particles that have peak emission in the orange before RTO. This was done by dispersing the etched particles in chloroform, which was then evaporated under dynamic vacuum with heating to 400 °C. Particles were then exposed to air for a short time (~1 min), still at 400 °C. They were then cooled under dynamic vacuum. Figure 9 shows the results of this rapid thermal oxidization procedure. For particles with original peak emission around 650 nm, after rapid thermal oxidization the peak emission shifted to 420 nm. The color change from orange to blue was accompanied by a slight increase in emission intensity. This process presumably causes the surface oxide layer on the particles to grow at the expense of the silicon core, decreasing the core size and shifting the emission wavelength toward the blue. However, the mechanism of this emission is far from understood, and we do not claim that the change in emission wavelength is directly due to quantum confine-
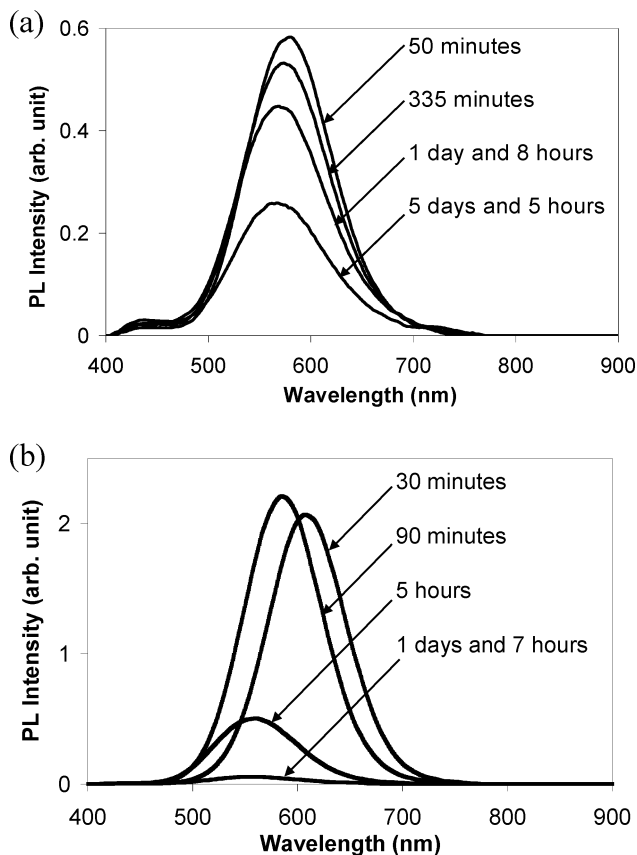
Figure 8. XPS spectrum for luminescent silicon particles. Analysis depth is 2 nm for this sample. The inset picture shows a Si/SiO$_2$ core shell structure consistent with the measured Si to O ratio.

Figure 9. Normalized PL spectrum of blue-emitting nanoparticles and of the orange-emitting nanoparticles from which the blue-emitting particles were prepared. The inset shows chloroform dispersions of particles before and after rapid thermal oxidation, with UV illumination from below.
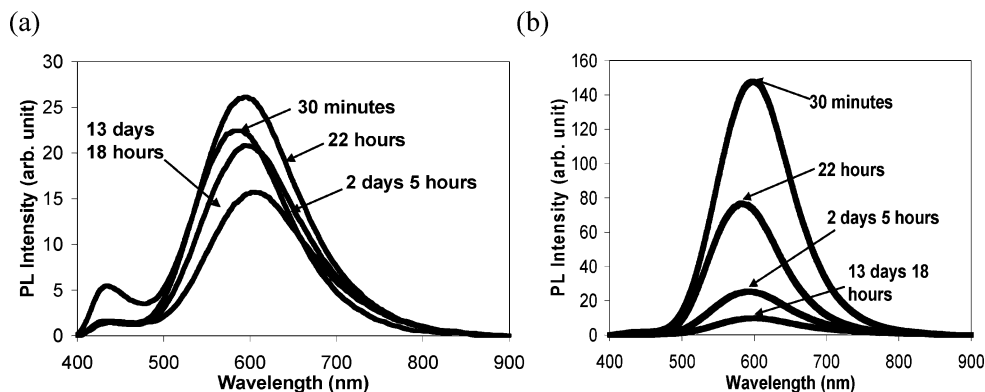
ment effects. In many cases, blue emission from Si particles is attributed to silicon suboxides, and this may also be the case here. This emission is not present if the particles are oxidized completely (at higher temperature or for longer times) to yield SiO$_2$ nanoparticles. In any case, producing blue-emitting particles in this manner allows us to have PL emission spanning the entire visible spectrum, with comparable brightness for a range of wavelengths. Subsequent studies will be required to determine the composition, crystallinity, and other properties of these blue-emitting particles, similar to what has been described above for the red-emitting particles.

d. Stability of the Silicon Nanoparticle Photoluminescence. A very important factor in the ultimate utility of these particles in applications and in investigations of their surface chemistry is the long-term stability of their optical properties. Lack of PL stability has significantly hampered applications of luminescent porous silicon. We have begun to explore the stability of the PL from these particles, and some of our initial observations are described here. Their behavior is generally consistent with observations on porous Si. Figure 10 shows the time dependence of the PL spectrum of dispersions of silicon nanoparticles in methanol and water. For the methanol dispersion shown in Figure 10a, the peak PL intensity dropped by a factor of 2.5 and the peak position shifted by about 12 nm toward the blue during the first 125 h after etching. A general trend seems to be that particles with initial emission at longer wavelengths show an initial increase in PL intensity with time, followed by a decrease in intensity at longer times, while particles with shorter wavelength emission show a monotonic decrease in PL intensity with time. However, this is not universally true

Figure 10. Change in PL emission spectrum with time after initial etching to produce luminescent particles: (a) particles dispersed in methanol; (b) particles dispersed in water.

for all our samples, and we continue to investigate the time evolution of the PL after etching. For water dispersions, the changes tend to be even larger. For the sample shown in Figure 10b, the peak position shifted by almost 50 nm toward the blue and the intensity decreased by almost two orders of magnitude during the first 31 h after preparation. The only powder sample for which we have seen significant change with time was one with an initial peak PL at 506 nm, which moved toward the red by about 40 nm during the first 2 days after preparation. Most of the powder samples have shown no significant change in PL intensity or wavelength after several weeks of storage at room temperature in air, under fluorescent room lighting. The changes in PL intensity and emission wavelength may result from slow (ultimately self-limiting) oxidation of the particles, producing a thicker oxide layer and smaller core diameter, or may result from other changes in the state of the particle surface. The mechanism of luminescence in these particles is not yet firmly es-

(a)　　　　　　　　　　　　　　　　　(b)

Figure 11. Time dependence of PL spectrum from silicon nanoparticles dispersed in chloroform after etching. The particles in (a) were washed for 1.5 min with 30% HNO_3 at the end of the etching procedure, while those in (b) were not. Note that the intensities cannot be compared directly between the two samples, due to differences in particle concentration, etc., but they can be compared quantitatively for the same sample at different times.

tablished, and therefore we can only speculate as to the source(s) of changes in it. We are currently investigating the stability of the PL further, and the surface treatment of the particles to stabilize their photoluminescence properties when dispersed in solvents. It should be emphasized that in the vast majority of samples, the changes in PL intensity described above have not led to a total loss of visible PL from the particles. We have many samples that, after 3 months of storage in air at room temperature exposed to room light, still show PL emission that is clearly visible to the unaided eye when excited by a 4-W handheld UV lamp.

e. Stabilizing PL of Silicon Nanoparticles by Wet Oxidation. One means of stabilizing the PL from these nanoparticles is surface oxidization using HNO_3 or another oxidizer in solution. Chemical oxidization of Si nanoparticles may provide a high quality, chemically inert, and relatively impermeable SiO_2 layer on the particle surface and therefore stabilize the emission by preventing further changes in the state of the particle surface. Initial results from this approach are quite promising. Figure 11 shows the PL from particles treated with 30% HNO_3 for 1.5 min immediately after etching, along with that from untreated particles. After about 13 days, the untreated particles in chloroform retained only about 6.5% of their initial emission intensity, while the particles oxidized with HNO_3 retained about 71% of their initial intensity.

f. Stability of Colloidal Dispersions of Silicon Nanoparticles. Furthermore, the dispersions shown in Figure 4 are not truly stable colloidal dispersions. While the particles are easily dispersed into water, methanol, and other small alcohols after etching by shaking or mild sonication, they visibly agglomerate and partially settle out of these solvents over a period of several hours to several days at room temperature, and a period of minutes to a few hours at 80 °C. By contrast, dispersions in 1,4-butanediol, 1,2-propanediol, and glycerol appear to be truly stable colloidal dispersions. These do not visibly agglomerate overnight at 80 °C or during several weeks of storage at room temperature. Quantitative measurements of degree of agglomeration (for example, using laser light scattering) have not been performed, but there is a clear qualitative difference between the dispersions that remain clear and those in which agglomeration occurs. Work to modify the particles' surfaces, not only to stabilize the PL but also to make them more readily dispersable in a wider range of solvents, is ongoing and will be reported separately. The chemistry of both Si and SiO_2 surfaces has been extensively studied, and thus we can use known strategies such as hydrosilylation of Si and reaction of alkoxysilanes

with SiO_2 to functionalize the particle surfaces. The ability to rapidly produce macroscopic samples of luminescent Si nanoparticles is allowing us to screen a large number of potential reagents. This has often not been possible with Si nanoparticles produced in much smaller quantities by other methods.

4. Summary and Conclusions

Silicon nanoparticles with an average diameter of about 5 nm were prepared by CO_2 laser driven pyrolysis of silane (photothermal aerosol synthesis). After HF/HNO_3 etching, silicon particles with controlled visible luminescence were produced. The wavelength of maximum PL emission from the nanoparticles can be controlled from above 800 nm to below 500 nm by controlling the etching time and conditions. The luminescent particles were characterized by XRD, FTIR, and XPS. The results confirmed that crystalline silicon structures are present in both the original and etched particles. The expected XRD peak broadening with decreasing particle size was observed. Rapid thermal oxidization of orange-emitting particles produced blue-emitting particles with peak PL emission near 420 nm. This method is unique in being able to produce macroscopic quantities (up to a few hundred milligrams in a few hours in our small bench-scale implementation) of Si nanoparticles with bright visible photoluminescence. Si nanoparticle dispersions in water and methanol with bright visible PL were also produced and characterized. These dispersions usually exhibited blue shift in their PL spectra with time as well as changes in PL intensity for the first few days after preparation. PL from powder samples was generally stable with time, except for some samples with green emission, for which the PL tended to shift toward the red with time. The PL from particles after etching can be stabilized significantly by chemical oxidization using HNO_3. The particles produce stable colloidal dispersions in diols and triols, but not in other solvents investigated so far. Additional efforts are needed, and are underway, to modify the particle surfaces to further stabilize the PL and to make them dispersable in a wide range of solvents.